

Lucidone protects human skin keratinocytes against free radical-induced oxidative damage and inflammation through the up-regulation of HO-1/Nrf2 antioxidant genes and down-regulation of NF- κ B signaling pathway



K.J. Senthil Kumar^{a,1}, Hsin-Ling Yang^{b,1}, Yu-Cheng Tsai^a, Pin-Chun Hung^b, Show-Huei Chang^a, Heng-Wei Lo^a, Pei-Chun Shen^a, Ssu-Ching Chen^c, Hui-Min Wang^d, Sheng-Yang Wang^e, Chih-Wei Chou^{a,*}, You-Cheng Hseu^{a,*}

^a Department of Cosmeceutics, College of Pharmacy, China Medical University, Taichung 40402, Taiwan

^b Institute of Nutrition, College of Health Care, China Medical University, Taichung 40402, Taiwan

^c Department of Life Sciences, National Central University, Chung Li 32001, Taiwan

^d Department of Fragrance and Cosmetic Science, Kaohsiung Medical University, Kaohsiung 80708, Taiwan

^e Department of Forestry, College of Agriculture and Natural Resources, National Chung Hsing University, Taichung 40227, Taiwan

ARTICLE INFO

Article history:

Received 10 January 2013

Accepted 30 April 2013

Available online 24 May 2013

Keywords:

Lindera erythrocarpa

Lucidone

Antioxidant

Anti-inflammation

Nrf2

ABSTRACT

We investigated the protective effects of lucidone, a naturally occurring cyclopentenone isolated from the fruits of *Lindera erythrocarpa* Makino, against free-radical and inflammation stimulator 2,2'-azobis (2-amidinopropane) dihydrochloride (AAPH)-induced oxidative stress in human keratinocyte (HaCaT) cells, with the aim of revealing the possible mechanisms underlying the protective efficacy. Lucidone pretreatment (0.5–10 μ g/mL) markedly increased HaCaT cell viability and suppressed AAPH-induced reactive oxygen species (ROS) generation, lipid peroxidation, and DNA damage. Notably, the antioxidant potential of lucidone was directly correlated with the increased expression of an antioxidant gene, heme oxygenase 1 (HO-1), which was followed by the augmentation of the nuclear translocation and transcriptional activation of NF-E2-related factor-2 (Nrf2), with or without AAPH. Nrf2 knockdown diminished the protective effects of lucidone. We also observed that lucidone pretreatment inhibited AAPH-induced inflammatory chemokine prostaglandin E₂ (PGE₂) production and the expression of cyclooxygenase-2 (COX-2) in HaCaT cells. Lucidone treatment also significantly inhibited AAPH-induced nuclear factor- κ B (NF- κ B) activation and suppressing the degradation of inhibitor- κ B (I- κ B). Furthermore, lucidone significantly diminished AAPH-induced COX-2 expression through the down-regulation of the extracellular signal-regulated kinase (ERK) and p38 MAPK signaling pathways. Therefore, lucidone may possess antioxidant and anti-inflammatory properties and may be useful for the prevention of free radical-induced skin damage.

© 2013 Elsevier Ltd. All rights reserved.

1. Introduction

Skin is the largest organ in the body, and one of its main functions is to protect the body from noxious substances, whether they are toxic chemicals or ultraviolet radiation, which result in skin aging, inflammation, and cancer (English et al., 2003). In the skin, free radicals are formed inside or around skin cells after exposure to ultraviolet radiation and by migrating inflammatory cells; in mitochondria, the oxidative stress imposed by these oxygen

species during respiration is known to damage skin cells (Muta-Takada et al., 2009; Rijnkels et al., 2003; Scharffetter-Kochanek et al., 1997; Vessey et al., 1992). In biological systems, free radicals can be generated in the form of ROS, such as superoxide anion, hydroxyl radical, hydrogen peroxide, singlet oxygen, nitric oxide, and peroxynitrites (Halliwell, 2007). These ROS cause destructive and irreversible damage to cellular components, including lipids, proteins, DNA, and other macromolecules (Kregel and Zhang, 2007). Although the inhibition of ROS-induced oxidative stress may contribute to the prevention of skin diseases, to date, very few substances or extracts have been demonstrated to be capable of protecting against ROS-induced skin injury (Svobodova et al., 2007).

* Corresponding authors. Tel.: +886 4 22053366x5308; fax: +886 4 22078083.

E-mail addresses: cwchou@mail.cmu.edu.tw (C.-W. Chou), yhseu@mail.cmu.edu.tw (Y.-C. Hseu).

¹ These authors are contributed equally to this work.

Several lines of evidence indicate that ROS participate in inflammation (Gilston et al., 2000; Rada et al., 2011). During inflammation, activated skin, vascular, smooth muscle, and macrophage cells produce a large amount of pro-inflammatory molecules, including inflammatory cytokines and chemokines (Fujiwara and Kobayashi, 2005; Saveria et al., 2006; Spagnoli et al., 2007), and the continual production of these pro-inflammatory molecules is involved in a variety of diseases, such as rheumatoid arthritis, atherosclerosis, asthma, pulmonary fibrosis, and cancer (McCulloch et al., 2006). Furthermore, the acute inflammation induced by sunburn induces erythema and skin cancer (Matsumura and Ananthaswamy, 2004). The pro-inflammatory mediators inducible nitric oxide synthase (iNOS) and COX-2 are responsible for the production of nitric oxide (NO) and PGE₂, respectively, and these enzymes play a pivotal role in the promotion of inflammation (Surh, 2003). NF- κ B is a transcription factor that is a key molecule in inflammation, and the expression of iNOS and COX-2 is directly coupled with up-regulation of NF- κ B (Surh, 2003). Under normal physiological conditions, NF- κ B is localized in the cytoplasm and tethered to its inhibitor protein, I- κ B. Upon activation by a variety of external stimuli, including bacterial lipopolysaccharide (LPS), I- κ B is phosphorylated and degraded via the proteasomal degradation pathway. This event further leads to release of NF- κ B, which then translocates to the nucleus and binds to its promoter region (κ B binding site) to increase the expression of a number of genes, including iNOS and COX-2 (Surh, 2003). In addition, mitogen-activated protein kinases (MAPKs), such as ERK1/2, p38, and c-jun N-terminal kinase1/2 (JNK1/2), are components of the inflammatory signal transduction pathways that also regulate iNOS and COX-2 expression in a variety of cells through the activation of NF- κ B (Kundu and Surh, 2005).

Previous studies have reported that AAPH induces oxidative stress through the intracellular elevation of ROS in a variety of cells, including macrophages, erythrocytes, and keratinocytes (Cui et al., 2004; Roche et al., 2009; Zhang et al., 2011). Furthermore, AAPH-induced ROS generation in various *in vitro* systems has been widely used for the study/screening of antioxidant ingredients in cosmetics (Yokozawa et al., 2000). During oxidative stress, the Nrf2 transcription factor is activated, inducing many antioxidant defense mechanism to mitigate oxidative damage and maintain the cellular redox homeostasis (Kaspar et al., 2009). Under un-stimulated conditions, Nrf2 is negatively regulated by Kelch-like ECH-associated protein 1 (Keap1), which facilitates the degradation of Nrf2 through ubiquitinated proteasomal degradation (Surh, 2003). Upon stimulation, Nrf2 translocates to the nucleus and recruits the small Maf (sMaf) protein. The Nrf2-sMaf heterodimer then binds to antioxidant response elements (AREs), a *cis*-acting DNA regulatory element, to activate the promoter region of many genes encoding phase II detoxification enzymes and antioxidants, such as heme oxygenase 1 (HO-1), peroxiredoxin 1 (PRX1), NAD(P)H quinone oxidoreductase 1 (NQO1), and glutamate-cysteine ligase (Kim et al., 2010). An important role of these antioxidant enzymes is to protect cells against the harmful effects of the free radicals that are produced during normal oxygen metabolism. It has been demonstrated that the Nrf2/ARE-mediated expression of HO-1 is induced by various external stimuli and plant-derived polyphenols (Surh, 2003).

Lindera erythrocarpa Makino (Lauraceae) is a deciduous shrub that is widely distributed in China, Japan, Korea, and Taiwan. The dried fruits (also known as red mountain pepper in English and hongguo shanhujiào in Chinese) are used in folk medicine as a digestive and anodyne drug (Ichino et al., 1988). The dried fruits are also a source of hot pepper flavor and are often used as a spice ingredient in Chinese cuisine (Fan et al., 2005). Lucidone is a naturally occurring cyclopentenone and was initially isolated from the fruits of *Lindera lucida* (Lauraceae) and subsequently from other species, including *L. erythrocarpa* (Senthil Kumar et al.,

2010). It has been reported that lucidone inhibited human farnesyl protein transferase activity, with an IC₅₀ value of 40 ± 3.5 μ M (Oh et al., 2005). The anti-inflammatory activity of *L. erythrocarpa* fruits has also been preliminarily evaluated by our team. Four anti-inflammatory cyclopentenones were identified by bioactivity-guided fractionation, with lucidone being the strongest inhibitor of NO production. Additionally, lucidone was also shown to be a potent anti-inflammatory agent in a croton oil-induced mouse ear edema assay (Wang et al., 2008). Our previous studies revealed that lucidone inhibits LPS-induced inflammation through the down-regulation of the NF- κ B and AP-1 signaling pathways *in vitro* and *in vivo* (Senthil Kumar et al., 2010; Senthil Kumar and Wang, 2009). Recently, we reported that lucidone showed hepatoprotective effects against alcohol-induced oxidative stress in liver cells through the up-regulation of the Nrf2 signaling pathway (Senthil Kumar et al., 2012).

In recent years, much attention has focused on certain dietary polyphenols in an attempt to repair photo-damaged skin as a means of preventing degeneration into free radical-induced skin diseases (Syed et al., 2006). However, the inhibitory effects of lucidone in AAPH-induced skin cell damage have not been well defined. Indeed, antioxidants that prevent free radical-induced skin damage are worthy of further investigation. In the present study, we investigated the protective mechanisms of lucidone in AAPH-treated human keratinocyte-derived HaCaT cells. It was found that lucidone could attenuate AAPH-induced oxidative damage in keratinocytes by inhibiting ROS generation. These results suggest that lucidone could be a potential agent in the treatment of skin-related diseases.

2. Materials and methods

2.1. Chemicals and reagents

Dulbecco's modified Eagle medium (DMEM), fetal bovine serum (FBS), glutamine, and penicillin/streptomycin were purchased from Invitrogen/GIBCO BRL (Grand Island, NY). AAPH, 3-(4,5-dimethylthiazol-2-yl)-2,5-diphenyltetrazolium bromide (MTT), and 2',7'-dihydrofluorescein-diacetate (DCFH-DA) were purchased from Sigma-Aldrich (St. Louis, MO). Antibodies against Nrf2, COX-2, NF- κ B, I- κ B α , and β -actin were obtained from Santa Cruz Biotechnology Inc. (Heidelberg, Germany). Anti-rabbit polyclonal HO-1 antibody was purchased from Abcam (Cambridge, UK). Antibodies against phospho-ERK1/2, phospho-p38, and phospho-JNK were obtained from Cell Signaling Technology Inc. (Danvers, MA). 4',6-Diamidino-2-phenylindole dihydrochloride (DAPI) and inhibitors of ERK (PD98059), p38 (SB203580), and JNK (SP600125) were obtained from Calbiochem (La Jolla, CA). All other chemicals were of the highest grade commercially available and supplied by either Merck (Darmstadt, Germany) or Sigma Chemical Co.

2.2. Isolation and characterization of lucidone from the fruits of *L. erythrocarpa*

Lucidone was isolated from the fruits of *L. erythrocarpa* as described previously (Wang et al., 2008). Briefly, 2.0 kg of dried fruits was extracted with 2 L EtOH to produce an ethanolic extract. The total crude *L. erythrocarpa* extract was concentrated under vacuum to yield a residue (124.3 g). Then, 100 g of the crude residue was suspended in 100 mL distilled water and partitioned with *n*-hexane (*n*-hex) and ethyl acetate (EA), yielding an *n*-hex-soluble fraction, EA-soluble fraction, and EA-insoluble fraction, with total yields of 16.0%, 45.6%, and 34.3%, respectively. The biologically active EA-soluble fraction was further chromatographed using a silica gel (300 g) column, eluted with a gradient of *n*-hex/EA (95/5 to 100/0) to obtain a total of 12 subfractions (EA1–EA12). The active fraction (EA5) was further separated by semi-preparative high-performance liquid chromatography (HPLC) using a Cosmogel column (Comosil Co., 250 mm × 10 mm) eluted with an *n*-hex/dichloromethane/EA solvent system to obtain four major compounds: lucidone (1), *cis*/trans-methylucidone (2), methyl linderone (3), and linderone (4). The amount of active lucidone in the EtOH extract was further analyzed by HPLC, and the purity of lucidone of >99% was verified by HPLC and ¹H NMR. The chemical structure of lucidone is shown in Fig. 1A.

2.3. Cell culture and sample treatment

The immortalized human keratinocyte cell line HaCaT was kindly provided by Dr. Te-Chang Lee (Institute of Biomedical Sciences, Academia Sinica, Taiwan). The HaCaT cells were maintained at 37 °C in a humidified atmosphere of 95% air and

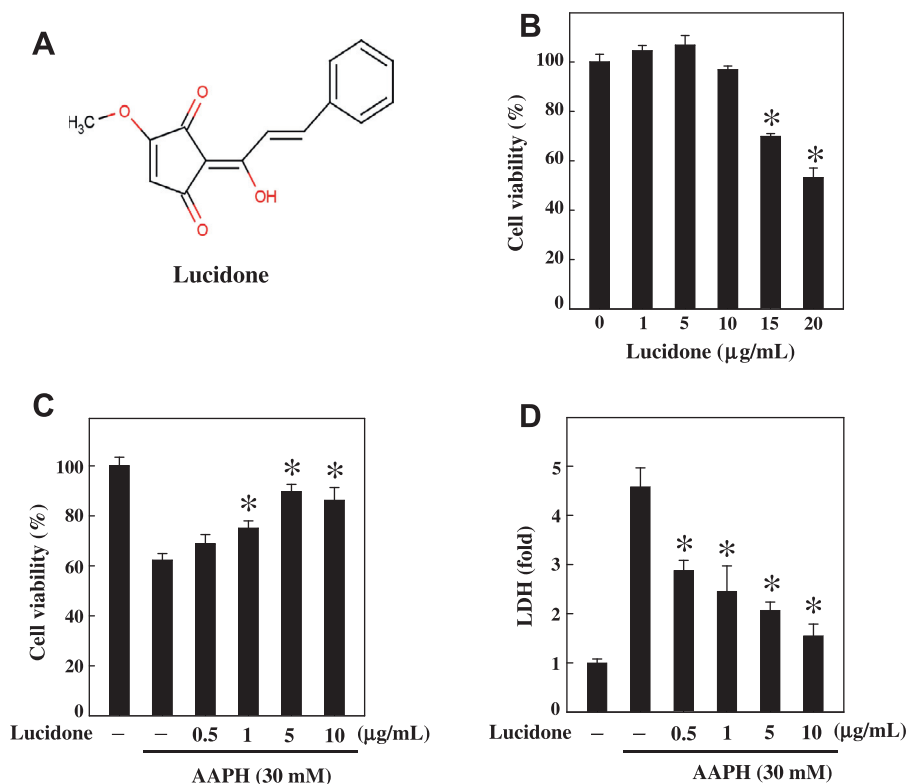


Fig. 1. Lucidone inhibits AAPH-induced cytotoxicity in human keratinocyte (HaCaT) cells. (A) Chemical structure of lucidone. The cells were pretreated with lucidone (0–20 µg/mL) for 24 h and then treated without (B) or with (C) AAPH (30 mM) for 6 h. The protective effects of lucidone were determined by the mitochondrial tetrazolium (MTT) assay. The cell viability (%) was calculated as follows: $(A_{570} \text{ of treated cells} / A_{570} \text{ of untreated cells}) \times 100$. (D) The LDH activity was measured as the LDH release from damaged membranes, as described in Section 2. The cells were pretreated with lucidone (0–10 µg/mL) for 24 h, and oxidative stress was stimulated by the addition of AAPH (30 mM) for 6 h. The results are the mean \pm SD of three independent assays. *Indicates a significant difference between the control (B) or AAPH-treated (C and D) group ($p < 0.05$).

5% CO₂ in DMEM medium supplemented with 10% heat-inactivated FBS, 2 mmol/L glutamine, and 1% penicillin/streptomycin. For the experiments, 1×10^5 cells/mL were seeded in a T-75 culture flask and maintained in a tissue culture incubator. The cells were pretreated with or without lucidone (0.5–10 µg/mL) for 24 h prior to the stimulation of oxidative stress by AAPH. The HaCaT cells were then exposed to 30 mM AAPH for the indicated times. The water-soluble free-radical generator AAPH was used to induce oxidative stress *in vitro*, and peroxy radicals were generated by the thermal decomposition of the azo compound in the presence of oxygen. In additional experiments, the cells were pretreated with an ERK inhibitor (PD98059; 30 µM), p38 inhibitor (SB203580; 30 µM), or JNK inhibitor (SP600125; 30 µM) for 1 h and then treated with AAPH (30 mM) for 4 h.

2.4. MTT assay

The effect of lucidone on cell viability was monitored using the MTT colorimetric assay. In brief, after an overnight incubation, HaCaT cells at a density of 2×10^5 cells/well in 12-well plates were pretreated with various concentrations of lucidone (0.5–20 µg/mL) for 24 h and then incubated with 30 mM AAPH for 6 h. After treatment, the cells were incubated with 400 µL 0.5 mg/mL MTT in phosphate buffered saline (PBS) for 2 h. The culture supernatant was removed, and the MTT formazan crystals were dissolved with 400 µL isopropanol; the absorbance was measured at 570 nm using an enzyme-linked immunosorbent assay (ELISA) reader (Bio-Tek Instruments, Winooski, VT). The effect of lucidone on cell viability was assessed as the percent of viable cells compared with the vehicle-treated control cells, which were arbitrarily assigned a viability of 100%. The assay was performed in triplicate at each concentration.

2.5. Lactate dehydrogenase (LDH) release assay

The activity of LDH released into the culture medium through damaged membranes was measured spectrophotometrically using the LDH cytotoxicity assay kit from Roche Diagnostics (Mannheim, Germany), as described previously (Chao et al., 2010). The method is based on the LDH-catalyzed reduction of pyruvate to lactate by an equimolar amount of nicotinamide adenine dinucleotide (NADH); NADH formation is detected by the release of a chromogen that emits at 450–490 nm. After lucidone treatment (0.5–10 µg/mL) for 24 h, the cells were stimu-

lated with AAPH (30 mM) for 6 h in serum-free medium. An equal amount of culture supernatant was mixed with fresh LDH buffer [50 mM Na₂HPO₄ and 1.22 mM sodium pyruvate (pH 7.5)] containing NADH (0.33 g/L) in a microplate, and the decrease in absorbance was monitored.

2.6. Measurement of ROS generation

The intracellular accumulation of ROS was detected by fluorescence microscopy using DCFH-DA. The HaCaT cells (2×10^5 cells/well) were cultured in a 12-well plate in DMEM supplemented with 10% FBS; the culture medium was renewed when the cells reached 80% confluence. After lucidone treatment (0.5–10 µg/mL) for 24 h and AAPH treatment (30 mM) for 6 h, the cells were incubated with 10 µM DCFH-DA in the culture medium at 37 °C for 30 min, whereby the acetate groups on DCFH-DA were removed by an intracellular esterase, trapping the probe inside the cells. The cells were then washed with warm PBS buffer. ROS production can be measured by the changes in fluorescence due to the intracellular accumulation of 2',7'-dihydrofluorescein (DCF) caused by the oxidation of DCFH. The DCF fluorescence was measured using a fluorescence microscope (Olympus 1 × 71 at 200× magnification). The fluorescence intensity under each condition was quantified using a squared section of fluorescence-stained cells with analySIS LS 5.0 soft image solution (Olympus Imaging America Inc., Corporate Parkway Centre Valley, PA), and the percentage of fluorescence intensity (ROS generation) was compared with that of the vehicle-treated control cells, which were arbitrarily assigned a value of 100%.

2.7. Measurement of lipid peroxidation

To estimate the amount of lipid peroxidation, the levels of malondialdehyde (MDA) equivalents in the HaCaT cells were determined using the thiobarbituric acid reactive substances (TBARS) assay, as described previously (Camera et al., 2009). Briefly, HaCaT cells at a density of 2×10^5 cells/well in 12-well plates were pretreated with lucidone (0.5–10 µg/mL) for 24 h and then challenged with AAPH (30 mM) for 6 h. The cell lysates were mixed with 1.5 mL 0.67% thiobarbituric acid (TBA) and 1.5 mL 20% trichloroacetic acid. The samples were then heated at 95 °C for 30 min, and the temperature of the reaction product was maintained at 25 °C for 30 min. The samples were then centrifuged at 860g for 15 min at 4 °C. TBA reacts

with the oxidative degradation products of lipids in samples, yielding red complexes that absorb at 532 nm, as measured using an ELISA microplate reader (Bio-Tek Instruments). The total protein content was determined by the Bradford method using the Bio-Rad protein assay reagent (Bio-Rad, Hercules, CA) with bovine serum albumin (BSA) as the standard. Freshly diluted tetra-ethoxypropane, which produces MDA, was used as a standard control. The results are expressed as mmol MDA/mg protein.

2.8. Comet assay (single-cell gel electrophoresis assay)

The assay was essentially the same as that described previously (Singh et al., 1988). Briefly, cells were pretreated with or without lucidone (0.5–10 µg/mL) for 24 h and then exposed to AAPH (30 mM) for 6 h. The treated HaCaT cells (1×10^6 cells/dish in a 10-cm dish) were suspended in 1% low-melting-point agarose in PBS (pH 7.4) and pipetted onto superfrosted glass microscope slides precoated with a layer of 1% normal-melting-point agarose (warmed at 37 °C prior to use). The agarose was allowed to set at 4 °C for 10 min before the slides were immersed in lysis solution [2.5 M NaCl, 100 mM EDTA, 10 mM Tris (pH 10.0), and 1% Triton X-100] at 4 °C for 1 h to remove the cellular proteins. The slides were then placed in single rows in a 30-cm-wide horizontal electrophoresis tank containing 300 mM NaOH and 1 mM EDTA (pH 13.0) at 4 °C for 20 min to allow the separation of the two DNA strands (alkaline unwinding). Electrophoresis was performed in the unwinding solution at 23 V (1 V/cm) and 300 mA for 15 min. The slides were then washed three times for 5 min each with 400 mM Tris (pH 7.0) at 4 °C before staining with PI (2.5 µg/mL). The PI-stained nucleoids were examined under a fluorescence microscope using a 510–550 nm excitation filter at a 400× magnification. The damage was not homogeneous, and the visual scoring of the cellular DNA on each slide was based on the characterization of 100 randomly selected nuclei/nucleoids. The DNA damage in the HaCaT cells, observed as double- and single-strand DNA breaks at alkali-labile sites, was analyzed under alkaline conditions (pH 13.0). The damage was not homogeneous, and the visual scoring of the cellular DNA on each slide was based on the characterization of 100 randomly selected nucleoids.

2.9. Preparation of whole, cytosolic, and nuclear extracts

HaCaT cells (1×10^6 cells/dish) in 10-cm dishes were grown in DMEM containing 10% FBS to a nearly confluent monolayer. The cells were pretreated with lucidone (0.5–10 µg/mL) for 24 h and exposed to AAPH (30 mM) for 6 h, washed with cold PBS. To obtain the total cell lysate, cell pellets were subsequently suspended in 100 µL lysis buffer containing 10 mM Tris-HCl, pH 8.0, 320 mM sucrose, 1% Triton X-100, 5 mM EDTA, 2 mM dithiothreitol and 1 mM phenylmethylsulfonyl fluoride. The suspensions were sonicated and kept on ice for 20 min, then centrifuged at 15,000g for 30 min at 4 °C. For the cytoplasmic and nuclear extracts, cell pellets were re-suspended in lysis buffer containing 10 mM HEPES (pH 8.0), 0.1 mM EDTA, 10 mM KCl, 100 µM EGTA, 1 mM DTT, 500 µM PMSF, 2.0 µg/mL leupeptin, 2.0 µg/mL aprotinin, and 500 µg/mL benzamidine. The cells were allowed to swell on ice for 15 min. NP-40 [10% (v/v), 15 µL] was subsequently added to the cell suspension. The samples were vortex every 5 min for 20 min. The homogenates were centrifuged for 5 min at 12,000g, and the supernatant was used as the cytosolic extract. The nuclear pellet was re-suspended in cold extraction buffer containing 20 mM HEPES (pH 8.0), 1 mM EDTA, 400 mM NaCl, 1 mM EGTA, 1 mM DTT, 1 mM PMSF, 2.0 µg/mL leupeptin, 20 µg/mL aprotinin, and 500 µg/mL benzamidine. The samples were centrifuged at 15,000g for 30 min, and the obtained supernatant was used as the nuclear extract. The cytoplasmic and nuclear protein content was determined by the Bio-Rad protein assay reagent using BSA as a standard. All the protein fractions were stored at –80 °C until use.

2.10. Western blot analysis

Equal amounts of the protein fractions were reconstituted in sample buffer (62 mM Tris-HCl, 2% SDS, 10% glycerol, and 5% β-mercaptoethanol), and the mixture was boiled at 97 °C for 6 min. Equal amounts (60 µg) of the denatured protein samples were loaded into each lane, separated by SDS-PAGE on a 8–15% polyacrylamide gradient gel, and then transferred overnight onto polyvinylidene difluoride membranes. The membranes were blocked with 5% non-fat dried milk in PBS containing 1% Tween-20 for 1 h at room temperature, followed by incubation with the primary antibodies overnight and either horseradish peroxidase-conjugated goat anti-rabbit or anti-mouse antibodies for 2 h. The blots were detected using the ImageQuant™ LAS 4000 mini (Fujifilm) with the SuperSignal West Pico chemiluminescence substrate (Thermo Scientific Inc., Rockford, IL). The western blot analyses with antibodies against Nrf2, HO-1, COX-2, NF-κB, I-κB, phos-ERK, phos-p38, and phos-JNK were performed as described previously.

2.11. Nrf2 immunofluorescence

HaCaT cells at a density of 2×10^4 cells/well were cultured in DMEM medium with 10% FBS in an eight-well glass Tek chamber and treated with various concentrations of lucidone (0.5–10 µg/mL) for 24 h. After the lucidone treatment, the cells were exposed to AAPH (30 mM) for 6 h, fixed with 2% paraformaldehyde for 15 min,

permeabilized with 0.1% Triton X-100 for 10 min, washed and blocked with 10% FBS in PBS, and then incubated for 2 h with an anti-Nrf2 primary antibody in 1.5% FBS. The cells were then incubated with FITC-conjugated (488 nm) secondary antibodies for 1 h in 6% bovine serum albumin. The cells were then stained with 1 µg/mL DAPI for 5 min. The stained cells were washed with PBS and visualized using a fluorescence microscope at a 400× magnification.

2.12. siRNA transfection

siRNA was transfected using Lipofectamine RNAiMAX (Invitrogen) according to the manufacturer's instructions. For the transfections, HaCaT cells were grown in DMEM medium containing 10% FBS and plated in 6-well plates to yield 40–60% confluence at the time of transfection. The next day, the culture medium was replaced with 500 µL Opti-MEM (Invitrogen), and the cells were transfected using the RNAiMAX transfection reagent (Invitrogen). For each transfection, 5 µL RNAiMAX was mixed with 250 µL Opti-MEM and incubated for 5 min at room temperature. In a separate tube, siRNA (100 pM for a final concentration of 100 nM in 1 mL of Opti-MEM) was added to 250 µL Opti-MEM, and the siRNA solution was added to the diluted RNAiMAX reagent. The resulting siRNA/RNAiMAX mixture (500 µL) was incubated for an additional 25 min at room temperature to allow complex formation. The solution was then added to the cells in 6-well plates, giving a final transfection volume of 1 mL. After incubation for 6 h, the transfection medium was replaced with 2 mL of standard growth medium, and the cells were cultured at 37 °C. The cells were replaced with growth medium after transfection for 24 h. After lucidone pre-treatment (10 µg/mL) for 24 h, the cells were exposed to AAPH (30 mM) for 6 h and then subjected to a Western blot analysis and the MTT assay.

2.13. Determination of PGE₂ production

The PGE₂ concentration of the culture medium was determined using an ELISA assay kit (R&D Systems, Minneapolis, MN) according to the manufacturer's protocol. HaCaT cells (2×10^5 cells/well in 12-well plates) were pretreated with lucidone (0.5–10 µg/mL) for 24 h and challenged with AAPH (30 mM) for 6 h. The culture supernatant (100 µL) was collected, and the PGE₂ concentration was determined using an ELISA microplate reader.

2.14. Statistics

The data are presented as the mean ± SD of at least three independent experiments ($n = 3$). A one-way ANOVA, followed by Dunnett's test, was performed to determine the significant differences between groups with the aid of SPSS software version 12.0 (SPSS, Chicago, IL). Statistical significance was defined as $p < 0.05$ for all the tests.

3. Results

In this study, human keratinocyte HaCaT cells were used to investigate the ability of lucidone (0.5–10 µg/mL or 1.95–39 µM) to protect against the oxidative stress and inflammation induced by the free-radical generator AAPH and to elucidate the molecular mechanisms involved.

3.1. Lucidone inhibits AAPH-induced cytotoxicity in HaCaT cells

The cytotoxic effects of AAPH and lucidone were determined using the MTT assay. The treatment of HaCaT cells with lucidone did not result in any cytotoxic effect up to the concentration of 10 µg/mL, whereas cell viability was dose-dependently decreased at concentrations higher than 10 µg/mL (Fig. 1B). Therefore, we utilized a lucidone concentration of ≤10 µg/mL in our ensuing experiments. As shown in Fig. 1C, treatment with AAPH (30 mM) significantly reduced cell viability up to 62.3%, whereas the AAPH-induced reduction of cell viability was dose-dependently protected by lucidone treatment ($p < 0.05$). These results clearly indicate that the exposure of HaCaT cells to lucidone confers a significant protective effect against AAPH. Furthermore, the AAPH-induced membrane damage of keratinocytes was assessed using the LDH assay (Fig. 1D). AAPH-treatment significantly increased LDH release (4.6 ± 0.4 -fold) into the culture medium, whereas lucidone pretreatment (0.5–10 µg/mL) significantly ($p < 0.05$) diminished the AAPH-induced release of LDH in a dose-dependent manner (Fig. 1D).

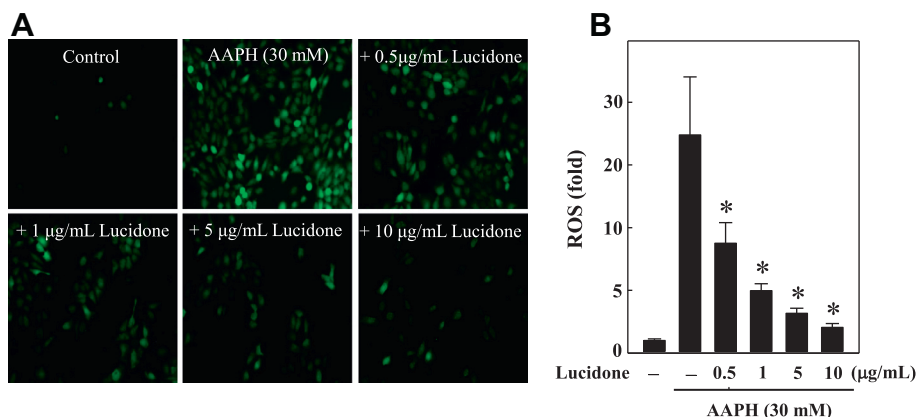
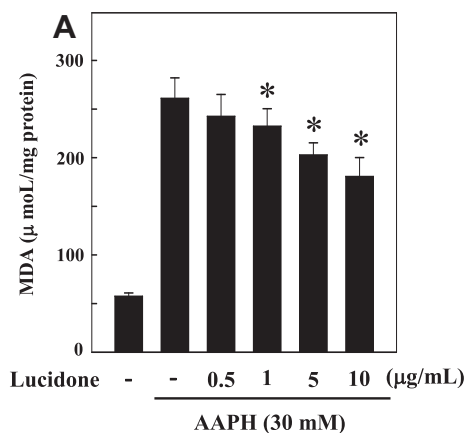


Fig. 2. Lucidone suppresses AAPH-induced ROS production in HaCaT cells. The cells were pre-incubated with or without lucidone (0–10 µg/mL) for 24 h and then stimulated with AAPH (30 mM) for 6 h. (A) The intracellular ROS level was indicated by DCF fluorescence and measured using fluorescence microscopy (200× magnification). The non-fluorescent, cell membrane-permeable probe DCFH-DA was added to the culture medium 30 min before the end of each experiment at a final concentration of 10 µM. DCFH-DA penetrates the cells, reacts with cellular ROS, and is metabolized into fluorescent DCF. (B) The percentage of the fluorescence intensity of the DCF-stained cells was quantified using Olympus soft image solution software for each condition, as described in Section 2. The results are the mean ± SD of three assays. *Indicates a significant difference in comparison to the AAPH-treated group ($p < 0.05$).



B

Group	Toxicity scale (%)					Total damage
	0	1	2	3	4	
Control	99 ± 1	1 ± 1	0 ± 0	0 ± 0	0 ± 0	1 ± 1
30 mM AAPH	1 ± 1	3 ± 4	14 ± 10	23 ± 4	59 ± 6	337 ± 5
+ 5 µg/mL Lucidone	22 ± 1	60 ± 8	18 ± 2	0 ± 0	0 ± 0	96 ± 2 *
+ 10 µg/mL Lucidone	24 ± 3	74 ± 2	2 ± 1	0 ± 0	0 ± 0	77 ± 1 *

Fig. 3. Lucidone suppresses AAPH-induced lipid peroxidation and DNA damage in HaCaT cells. The cells were pretreated with lucidone (0–10 µg/mL) for 24 h and then treated or not with AAPH (30 mM) for 6 h. (A) MDA production was measured using the TBARS assay, as described in Section 2. (B) The DNA damage in HaCaT cells was assessed using an alkaline comet assay. The cellular DNA was stained with DAPI and photographed under a fluorescence photomicroscope. The comet-like DNA formations were categorized into five classes (0, 1, 2, 3, or 4), representing increasing DNA damage observed as a “tail”. Each comet was assigned a value according to its class. The overall score for 100 comets ranged from 0 (100% of comets in class 0) to 400 (100% of comets in class 4). The observation and analysis of the results were always performed by the same experienced individual. The analysis was blinded, with the observer having no knowledge of the slide identity. The results are the mean ± SD of three assays. *Indicates a significant difference ($p < 0.05$) relative to the AAPH-treated groups.

3.2. Lucidone modulates AAPH-induced ROS generation in HaCaT cells

The intracellular ROS generation was monitored to investigate the role of oxidative stress in AAPH-treated HaCaT cells. The results obtained from the fluorescence microscopic analyses using DCFH-DA as a fluorescence probe demonstrated that the HaCaT cells

exposed to AAPH (30 mM) displayed significant increases in fluorescence (25.4 ± 7.8 -fold) as an indicator of intracellular ROS generation (Fig. 2A and B). However, the AAPH-induced increases of ROS generation were significantly ($p < 0.05$) inhibited by lucidone (0.5–10 µg/mL) in a dose-dependent manner (Fig. 2A and B). Therefore, presuming that the AAPH-induced reduction in cell viability is med-

iated by ROS generation, our results indicate that lucidone significantly suppressed AAPH-induced ROS generation in HaCaT cells.

3.3. Lucidone prevents AAPH-induced lipid peroxidation and DNA damage in HaCaT cells

AAPH-induced oxidative stress is also associated with the peroxidation of cellular lipids (Svobodova et al., 2007), which can be detected by measuring the intracellular levels of MDA (Camera et al., 2009). As shown in Fig. 3A, the level of MDA in the cell culture lysate dramatically increased in response to AAPH ($261 \pm 21 \mu\text{mol/mg}$ of protein), whereas lucidone pretreatment significantly inhibited the observed AAPH-induced MDA elevation in HaCaT cells. In addition, a lower or undetectable amount of MDA was observed in the cells pre-incubated with lucidone (data not shown). These results suggest that lucidone treatment significantly inhibits AAPH-induced oxidative stress in HaCaT cells, as directly evidenced by the reduction of the intracellular MDA levels.

DNA strand breakage is considered to be one of the most frequent damages induced by the free radical generator AAPH (Burcham and Harkin, 1999). The AAPH-induced formation of DNA strand breaks (DNA damage) in the cellular DNA was evaluated using single-cell gel electrophoresis (comet assay). In this study, we quantified the AAPH-induced DNA damage by means of a toxicity scale. AAPH exposure (30 mM) resulted in significant DNA damage, with the total damage being $337 \pm 5\%$ (Fig. 3B). However, this adverse effect was significantly ($p < 0.05$) inhibited by lucidone at concentrations of 5 and 10 $\mu\text{g/mL}$, reducing the total damage to $96 \pm 2\%$ and $77 \pm 1\%$, respectively (Fig. 3B). These data further support that lucidone pretreatment not only protects HaCaT cells from AAPH-induced oxidative stress but also prevents DNA damage.

3.4. Lucidone up-regulates HO-1 expression via Nrf2 activation in HaCaT cells

We hypothesized that the protective effects of lucidone against AAPH-induced oxidative stress result from the induction of antioxidant genes, such as HO-1 and its transcription factor Nrf2. As expected, we observed that lucidone (0.5–10 $\mu\text{g/mL}$) significantly increased HO-1 and Nrf2 expression in a dose-dependent manner (Fig. 4A). To explore the protective mechanism further, the cells were pre-incubated with lucidone (0.5–10 $\mu\text{g/mL}$ for 24 h), and oxidative stress was induced with AAPH (30 mM for 6 h). The results obtained from Western blotting showed that the total content of Nrf2 was slightly increased in the AAPH-induced cells and dramatically increased in response to the lucidone treatment after AAPH exposure (Fig. 4B). Moreover, as the downstream target of Nrf2, HO-1 protein expression was significantly and dose-dependently increased by lucidone in both the stimulated and unstimulated HaCaT cells (Fig. 4A and B). In addition, another antioxidant enzyme, zinc/copper-superoxide dismutase (Zn/Cu-SOD), was unaffected by neither AAPH nor lucidone (Fig. 4A and B). Furthermore, we hypothesized that the induction of HO-1 by lucidone is due to the nuclear translocation and transcriptional activation of Nrf2. Therefore, next we monitored the nuclear translocation of Nrf2 using an immunofluorescence assay. Fig. 4C shows that the nuclear accumulation of Nrf2 was significantly ($p < 0.05$) increased when the cells were pretreated with lucidone prior to AAPH exposure. In addition, the cytosolic Nrf2 levels were decreased in response to AAPH (30 mM) and lucidone (10 $\mu\text{g/mL}$) (Fig. 4C), strongly supporting the hypothesis that Nrf2 translocates to the nucleus after AAPH exposure and that lucidone facilitates this nuclear accumulation of Nrf2. The difference between the

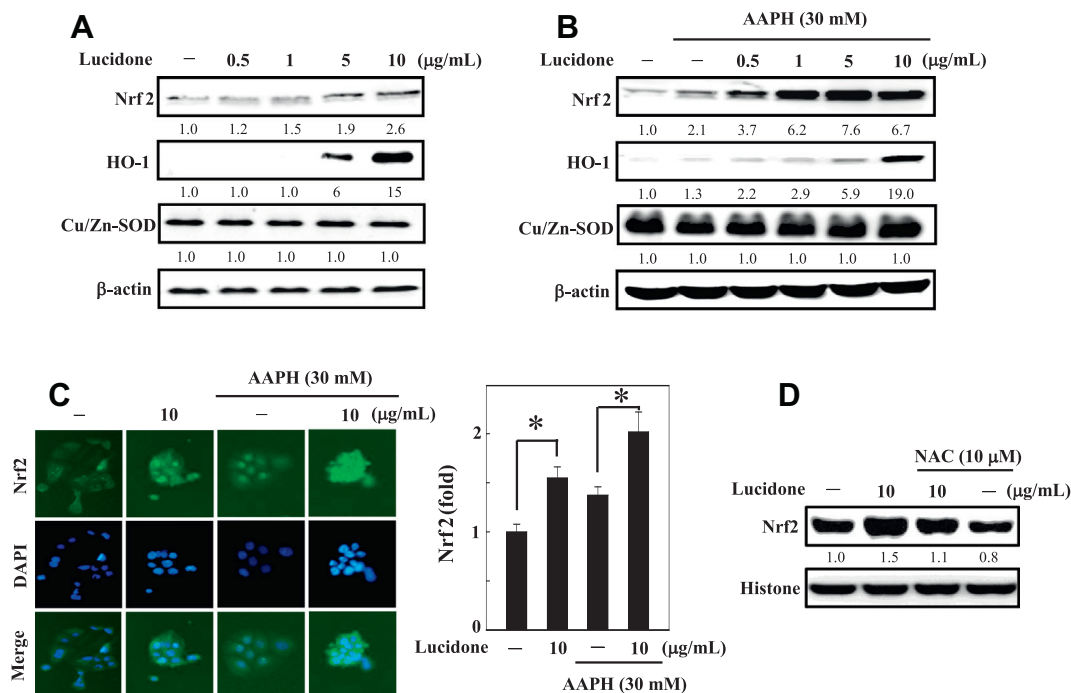


Fig. 4. Lucidone up-regulates the antioxidant markers HO-1 and Nrf2 in AAPH-treated HaCaT cells. The cells were pretreated with lucidone (0–10 $\mu\text{g/mL}$) for 24 h and then treated without (A) or with (B) AAPH (30 mM) for 6 h. The Western blot analysis shows the effects of lucidone on the total protein levels of Nrf2 and HO-1 in whole cells (A and B). An equal amount (50 μg) of total lysate from each sample was resolved by 8–15% SDS-PAGE, with β -actin as a control. The relative changes in the intensities of the protein bands were measured by densitometry. (C) Immunofluorescence staining shows the changes in Nrf2 levels in the HaCaT cells. The cells were pretreated with or without lucidone (10 $\mu\text{g/mL}$) for 24 h and then treated or not with AAPH (30 mM) for 6 h. The cells were stained with DAPI (1 $\mu\text{g/mL}$) for 5 min and examined using fluorescence microscopy (magnification 200 \times). The percentage of the fluorescence intensity of the cells was quantified using Olympus soft image solution software for each condition. (D) HaCaT cells were transfected with Nrf2 siRNA and pre-incubated with or without lucidone (10 $\mu\text{g/mL}$) in the presence or absence of NAC (10 μM) for 24 h, then the cells were stimulated by AAPH for 6 h. Nrf2 expression in the nuclear fraction was quantified by western blot analysis. The results are the mean \pm SD of three assays. *A significant difference in comparison to the control groups ($p < 0.05$).

lucidone-treated cells and AAPH-challenged cells was statistically significant, also indicating that lucidone promotes Nrf2 nuclear translocation in HaCaT cells. To further confirm the effect of NAC on lucidone-induced Nrf2 activation, HaCaT cells were pre-incubated with or without NAC in the presence or absence of lucidone for 6 h. Nrf2 protein levels in the nuclear extracts were measured by Western blotting. As shown in Fig. 4D, lucidone caused a significant increase in Nrf2 expression from 1-fold to 1.5-fold, whereas NAC co-treatment significantly inhibited the lucidone-induced Nrf2 activation from 1.5-fold to 1.1-fold.

3.5. Nrf2 knockdown diminishes the protective effect of lucidone in HaCaT cells

To demonstrate the importance of Nrf2 up-regulation, we developed an Nrf2 gene knockdown model in HaCaT cells using siRNA transfection. Cells were treated with control siRNA not affected the Nrf2 and HO-1 expression in HaCaT cells, whereas control siRNA and lucidone treatment significantly increased Nrf2 and HO-1 expression to 2.5-fold and 1.8-fold, respectively (Fig. 5A). The effect of knocking down of the Nrf2 gene was confirmed by Western blot analysis, which showed that the transfection of siNrf2 (100 pM) led to the reduction in the Nrf2 protein level to 0.3-fold and siNrf2 also could decreased the lucidone (10 μ g/mL)-induced Nrf2 expression in HaCaT cells (Fig. 5A). Nrf2 knockdown also significantly inhibited the protein expression of HO-1 in the HaCaT cells, which is evidence that the augmentation of HO-1 was

mediated by Nrf2 (Fig. 5A). However, the cell viability was not affected by either siNrf2 alone or in combination with lucidone (Fig. 5B). The knockdown of Nrf2 was effective even with lucidone treatment for 24 h, that is, siNrf2 transfection abrogated the protective effect of lucidone, and HaCaT cells did not survive a 30 mM dose of AAPH even in the presence of lucidone (Fig. 5B). To further confirm the involvement of Nrf2, the inhibitory effect of lucidone on AAPH-induced ROS generation was measured in Nrf2 knock-down HaCaT cells. Cells were transiently transfected with control or Nrf2 siRNA, then pre-incubated with or without lucidone for 24 h in the presence or absence of AAPH for 6 h. Compared to the control cells, Nrf2 knock-down significantly increased intracellular ROS level from 100% to $161 \pm 17\%$, whereas lucidone pretreatment slightly inhibited the AAPH-induced ROS generation in Nrf2 knock-down cells (Fig. 5C). This data provide a positive evidence that lucidone inhibits AAPH-induced ROS generation through the activation of Nrf2 signaling pathway.

3.6. Lucidone pre-treatment inhibits AAPH-induced PGE₂ production and COX-2 expression in HaCaT cells

PGE₂ represents the most important inflammatory product of COX-2 activity; thus, this prostaglandin was quantified in a cell-free culture supernatant (Liao et al., 2012). As shown in Fig. 6A, the cells stimulated with AAPH (30 mM) alone produced a significant amount of PGE₂ (600 ± 24 pg/mL), and the AAPH-induced elevation of PGE₂ production was significantly ($p < 0.05$) inhibited by

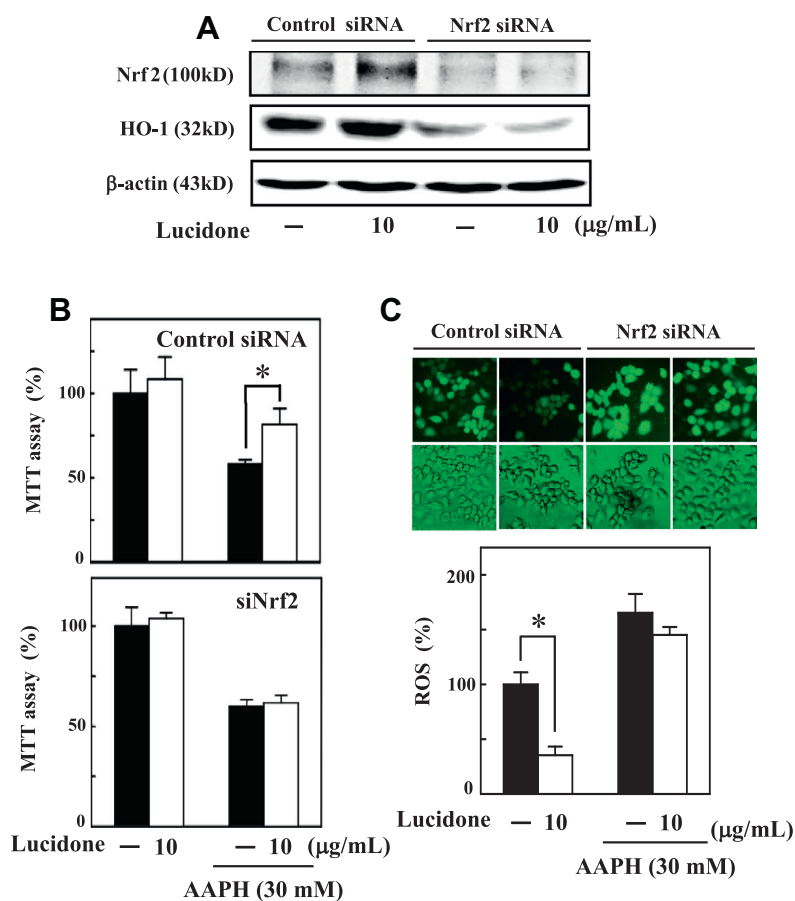


Fig. 5. Nrf2 siRNA attenuates the protective effect of lucidone. (A) HaCaT cells were transfected with a specific siRNA against Nrf2 or a non-silencing control siRNA. Following transfection for 24 h, the cells were incubated with or without lucidone (10 μ M) for 24 h, and the knockdown was evaluated by Western blotting. (B) The control and Nrf2 siRNA-treated HaCaT cells were incubated with or without lucidone (10 μ M) for 24 h and then treated or not with 30 mM AAPH for 6 h. The cell viability was determined using the MTT assay. (C) The intracellular ROS level was indicated by DCF fluorescence. Each value is expressed as the mean \pm SD ($n = 3$). *A significant difference in comparison to the control groups ($p < 0.05$).

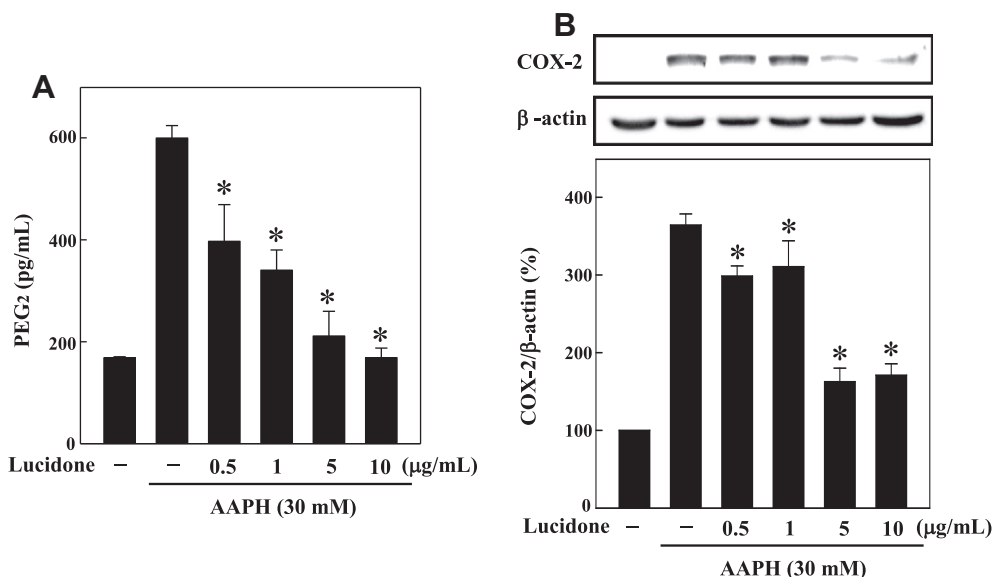


Fig. 6. Lucidone down-regulates PGE₂ production through the down-regulation of COX-2 expression in AAPH-treated HaCaT cells. The cells were pretreated with lucidone (0–10 μg/mL) for 24 h and then treated with or without AAPH (30 mM) for 6 h. (A) PGE₂ production was measured using a commercially available EIA kit, as described in Section 2. (B) The COX-2 protein expression was measured by Western blot analysis. Protein (50 μg) from each sample was resolved using 10% SDS–PAGE. The levels of COX-2 proteins in the cell lysates were analyzed using an antibody specific for COX-2, and β-actin was used as an internal control for the sample loading. The relative changes in the protein bands were measured by a densitometric analysis in which the control was 1.0-fold, as shown immediately below the gel data. The photomicrographs shown are from one representative experiment repeated twice, with similar results. *Indicates a significant difference in comparison to the AAPH-treated group ($p < 0.05$).

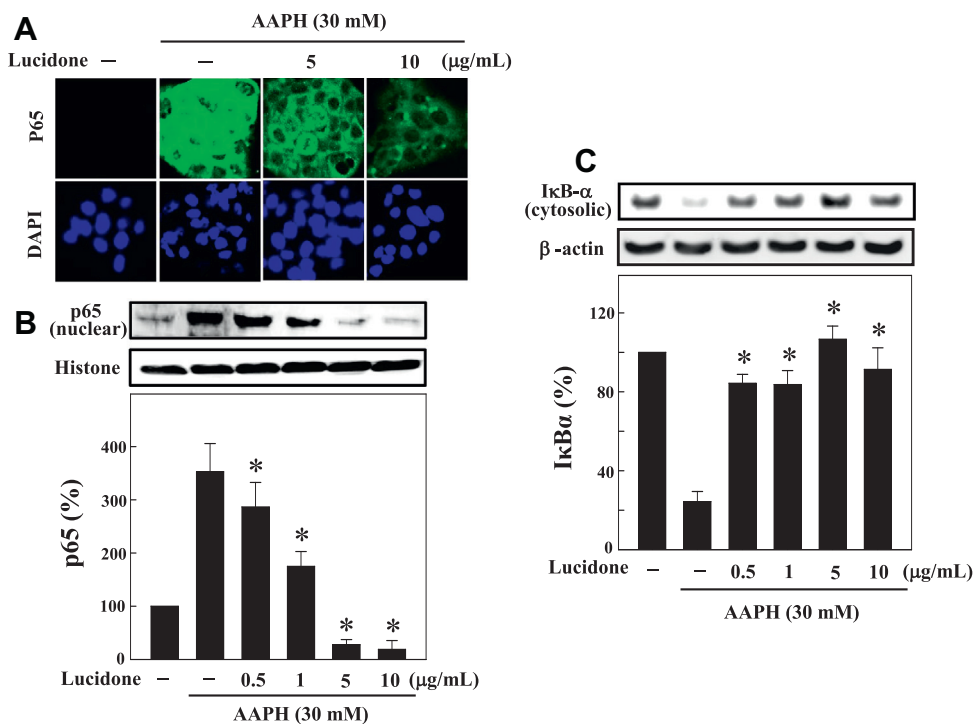


Fig. 7. Lucidone down-regulates nuclear NF-κB translocation through the suppression IκB degradation in AAPH-treated HaCaT cells. (A) Immunofluorescence staining shows the changes in NF-κB in HaCaT cells. The cells were pretreated with or without lucidone (5 and 10 μg/mL) for 24 h and then treated or not with AAPH (30 mM) for 6 h. The cells were stained with DAPI (1 μg/mL) for 5 min and examined by fluorescence microscopy (magnification 400×). (B and C) The cells were pretreated with lucidone (0–10 μg/mL) for 24 h and then treated with or without AAPH (30 mM) for 6 h. Protein (50 μg) from each sample was resolved using 10% SDS–PAGE, and Western blotting was performed. The nuclear protein level of p65 (B) and IκBα (C) protein level in cytoplasm was measured using specific nuclear and cytoplasmic extracts. Histone and β-actin were used as an internal control for nuclear and cytoplasmic extracts, respectively. The relative changes in the protein bands were measured by a densitometric analysis in which the control was 1.0-fold, as shown immediately below the gel data. The photomicrographs shown are from one representative experiment repeated twice, with similar results. *Indicates a significant difference in comparison to the AAPH-treated group ($p < 0.05$).

lucidone pretreatment (0.5–10 μg/mL) (Fig. 6A). Moreover, for the cells incubated with lucidone alone (0.5–10 μg/mL), the amount of PGE₂ in the culture medium was maintained at a background level

similar to that for the un-stimulated samples (data not shown). To confirm this effect, we examined the COX-2 protein expression level using Western blot analysis, which showed that AAPH

treatment significantly augmented COX-2 expression in HaCaT cells (Fig. 6B); this expression was markedly ($p < 0.05$) attenuated in the cells pre-treated with lucidone (0.5–10 $\mu\text{g}/\text{mL}$) in a dose-dependent manner (Fig. 6B).

3.7. Lucidone prevents I- κ B α degradation and NF- κ B activation in AAPH-induced HaCaT cells

NF- κ B activation is a critical event for the activation of several inflammatory genes, including iNOS and COX-2 (Kundu and Surh, 2005). The effect of lucidone on AAPH-induced NF- κ B activation in HaCaT cells was examined by immunofluorescence and Western blot analysis. As shown in Fig. 7A, compare to control, the nuclear accumulation of NF- κ B was markedly increased by AAPH, whereas lucidone treatment significantly inhibited the AAPH-induced NF- κ B expression and nuclear accumulation in HaCaT cells. Further western blot analysis with nuclear extracts confirmed that the AAPH-induced nuclear translocation was significantly inhibited by lucidone in a dose-dependent manner (Fig. 7B). The phosphorylation and subsequent proteasomal degradation of I- κ B α is a critical step for the import of NF- κ B subunits into the nucleus (Kundu and Surh, 2005). Therefore, we examined the effect of lucidone on AAPH-induced NF- κ B activation in HaCaT cells via the detection of I- κ B α protein stability by Western blotting. The amount of I- κ B α protein was remarkably reduced in the cells exposed to AAPH (30 mM), whereas lucidone treatment (0.5–10 $\mu\text{g}/\text{mL}$) significantly ($p < 0.05$) prevented AAPH-induced I- κ B α degradation in a dose-dependent manner (Fig. 7C).

3.8. Lucidone attenuates AAPH-induced MAPK activation in HaCaT cells

It is well established that the mitogen-activated protein kinase (MAPK) pathway plays a major role in ultraviolet B-induced (Chen

et al., 2001) and LPS-induced (Ding et al., 2012) COX-2 expression in human keratinocytes. Moreover, MAPKs are also involved in the activation of NF- κ B (Kundu and Surh, 2005). To determine whether the inhibition of NF- κ B activation by lucidone was mediated by the MAPK pathway, we investigated the AAPH (30 mM)-induced phosphorylation of MAPK family proteins, particularly ERK, p38 MAPK, and JNK, in HaCaT cells using Western blot analyses. As shown in Fig. 8A, AAPH caused an increase in the phosphorylation of ERK, p38 MAPK, and JNK in HaCaT cells, whereas pretreatment with lucidone significantly ($p < 0.05$) suppressed this phosphorylation (Fig. 8A). These results clearly demonstrate that MAPKs are activated by AAPH and that this activation was significantly prevented by lucidone in HaCaT cells. To further elucidate the potential involvement of MAPKs, including the ERK, p38 MAPK, and JNK pathways, in AAPH-induced inflammation, the expression of the inflammatory marker gene COX-2 was analyzed by Western blotting. The HaCaT cells were pretreated with 30 μM ERK inhibitor PD98059, p38 MAPK inhibitor SB202190, or JNK inhibitor SP600125 for 1 h and incubated with or without AAPH for another 4 h, and the cell lysates were analyzed for COX-2 expression and ERK, p38 MAPK, and JNK phosphorylation. The AAPH-induced phosphorylation of ERK (Fig. 8B) and p38 (Fig. 8C) was significantly blocked by PD98059 and SB202190, respectively. However, the JNK inhibitor SP600125 could not down-regulate the AAPH-induced COX-2 expression (Fig. 8D); indeed, the AAPH-induced COX-2 expression was significantly up-regulated by JNK inhibitor SP600125 (Fig. 8D). These data indicate that the AAPH-mediated induction of COX-2 involves the ERK and p38 MAPK pathways but not the JNK pathway.

4. Discussion

Chemical or UV exposure to skin cells results in the generation of ROS, which comprise a number of active metabolites, including

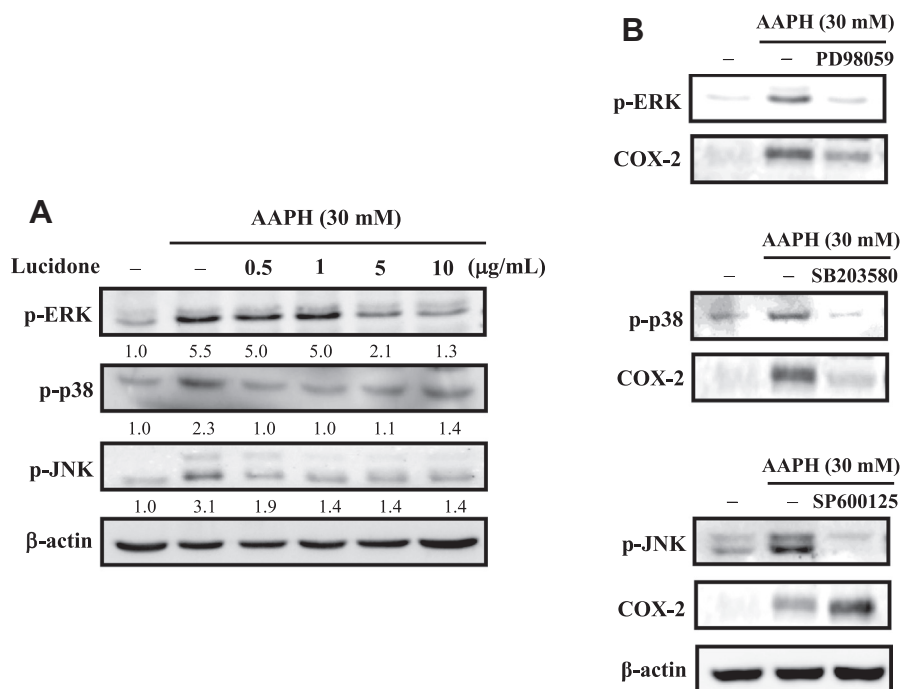


Fig. 8. Lucidone attenuates MAPK signaling pathways in AAPH-treated HaCaT cells. (A) The cells were pretreated with lucidone (0–10 $\mu\text{g}/\text{mL}$) for 24 h and then treated with or without AAPH (30 mM) for 4 h. The levels of phosphorylated ERK1/2 (p-ERK1/2), p38 (p-p38), and JNK1/2 (p-JNK1/2) were evaluated using phosphorylation-specific antibodies by Western blot analysis. (B) The lucidone-induced down-regulation of COX-2 expression is mediated by the ERK and p38 MAPK signaling pathways in AAPH-treated HaCaT cells. The cells were pretreated with ERK inhibitor (PD98059; 30 μM), p38 inhibitor (SB203580; 30 μM), or JNK inhibitor (SP600125; 30 μM) for 1 h and then treated with AAPH (30 mM) for 4 h. The COX-2 protein expression was measured using Western blot analysis. The proteins (50 μg) in each sample were resolved by 10% SDS-PAGE. The relative changes in the protein bands were measured by a densitometric analysis in which the control was 1.0-fold, as shown immediately below the gel data. The photomicrographs shown are from one representative experiment repeated twice, with similar results.

hydrogen radical, superoxide anion, peroxy radical, and their active precursors, namely singlet oxygen, hydrogen peroxide, and ozone (Cui et al., 2004; Svobodova et al., 2003). ROS damage cell membranes through the peroxidation of the fatty acids in the phospholipid cell membrane, producing lipid peroxides that are comparatively longer-lived species than ROS and can initiate the chain reactions that enhance the oxidative damage to the cells (Sharma et al., 2012). ROS are frequently generated in keratinocytes and fibroblasts and are rapidly removed by non-enzymatic and enzymatic antioxidants. It has been proposed that ROS-induced cellular injury is exaggerated with advanced photo-aging and skin diseases (Kregel and Zhang, 2007), with studies showing that antioxidant administration prevents skin cells from photo-aging. Therefore, we used an AAPH-based model to induce oxidative stress and cellular damage, which is similar to the inflammatory response, and investigated the protective effects of lucidone. The harmful effects of oxidative stress on keratinocytes exposed to AAPH were markedly attenuated when the cells were pre-incubated with lucidone. Lucidone also increased cell survival, as measured by the cellular metabolic activity (MTT assay) and plasma membrane integrity (LDH assay).

The measurement of oxidative stress markers, such as the intracellular accumulation of ROS and lipid peroxidation, provided useful information about the potential protective effects of lucidone under the AAPH-induced oxidative stress condition. In the present study, we also found that AAPH, a hydrophilic free radical generator, markedly induced ROS generation in human keratinocyte HaCaT cells. AAPH was also found to reduce HaCaT cell viability, which is hypothesized to occur through ROS-mediated apoptosis. Our results were in strong agreement with those of Cui et al. (2004), reporting that AAPH-induced apoptosis in human keratinocytes is mediated by the aberrant generation intracellular ROS. The pretreatment of HaCaT cells with lucidone significantly protected against the AAPH-induced reduction in cell viability and inhibited ROS generation. Such an anti-oxidative effect of lucidone was also observed previously (Senthil Kumar et al., 2012) against ethanol-induced oxidative stress in liver cells, however the present study is more informative because it revealed that lucidone is also very effective in eliminating ROS in AAPH-treated skin cells.

Free radicals can cause irreversible damage many biomolecules, including lipids, which can be used as biomarkers of oxidative stress. The peroxidation of polyunsaturated fatty acids gives rise to a vast range of aldehyde and carbonyl compounds, some of which, e.g., malonyldialdehyde (MDA), diffuse rapidly in aqueous medium, whereas the lipophilic compounds remain in the lipid phase. Remarkably, the AAPH-induced accumulation of MDA in keratinocytes was significantly reduced by lucidone pretreatment. These findings further support our assumption that lucidone directly or indirectly interacts with ROS. A similar inhibitory effect of lucidone against ethanol-induced lipid peroxidation in human hepatic cells was reported previously (Senthil Kumar et al., 2012).

The inhibition of AAPH-induced ROS generation in HaCaT cells by the pre-incubation with lucidone may be due either to a direct antioxidant mechanism (free radical-scavenging activity) and/or an indirect antioxidant mechanism (modulation of the endogenous antioxidant enzymatic system). Accordingly, we examined the mechanisms of action associated with the protective effects of lucidone under the AAPH-induced oxidative stress condition by measuring the free radical-scavenging capacity of lucidone using the 2,2-diphenyl-1-picrylhydrazyl (DPPH) assay. Lucidone showed very low direct free radical-scavenging activity compared with the reference compound curcumin (data not shown). Therefore, we hypothesized that lucidone may augment the intracellular redox balance by altering the activities and protein expression of such endogenous antioxidant enzymes including HO-1.

It has been well demonstrated that HO-1 is a major antioxidant enzyme that plays a vital role in the defense against free radical-induced oxidative damage in human skin cells (Svobodova et al., 2003). Moreover, Nrf2, a basic leucine-zipper (bZIP) transcription factor has been shown to be involved in the induction of various detoxifying (phase II) enzymes and antioxidants (Surh, 2003). Previous studies have shown that increasing Nrf2 activity in keratinocytes is highly protective during chemical- and UV-induced oxidative stress (Schafer et al., 2012). Several investigations have shown that plant-derived chemical substances enhance Nrf2-dependent ARE activity and induce HO-1 expression in a variety of cells, including keratinocytes (Narayanan et al., 2006). Unsurprisingly, lucidone, a natural cyclopentenedione, up-regulates the antioxidant genes HO-1 and Nrf2 in human keratinocytes. Thus, lucidone mainly protects skin cells from AAPH-induced oxidative stress by elevating intracellular antioxidant enzymes via the enhanced accumulation of a transcription factor for antioxidant genes, Nrf2, and dramatically inducing the expression of antioxidant gene HO-1 following AAPH exposure. Furthermore, the protein expression of HO-1 and Nrf2 in the lucidone alone-treated cells was significantly increased, though a profound augmentation of HO-1 and Nrf2 was observed when the cells were challenged with AAPH. Indeed, our data confirmed that the lucidone-mediated up-regulation of HO-1 and Nrf2 is critically governed by oxidative stress in keratinocytes. The discovery of RNA interference has revolutionized approaches to elucidating specific gene functions and pathways (Narayanan et al., 2006). Notably, siRNA-mediated transcriptional silencing is conserved in mammalian cells and, thus, provides a means to inhibit specific mammalian gene functions (Narayanan et al., 2006). Our data show that the siRNA-mediated knockdown of Nrf2 expression leads to enhanced HaCaT cell death. However, lucidone failed to protect Nrf2-knocked down keratinocytes from AAPH-induced oxidative damage. These data undoubtedly prove that the protective effect of lucidone is mainly mediated by the activation of Nrf2. Previous *in vitro* studies also supports this observation that lucidone treatment up-regulates HO-1 activity through the transcriptional activation of Nrf2 in human hepatoma HepG2 and Ava5 cell lines (Senthil Kumar et al., 2012; Chen et al., 2013).

DNA damage is known to be one of the most sensitive biological markers for evaluating oxidative stress *in vitro* (Kim et al., 2012). Several lines of evidence show that the exposure of keratinocytes to free radical generators, including UV, AAPH, organic hydroxides, and alkylperoxides, results in DNA damage, particularly the oxidative modification of DNA bases and DNA strand breakage (Cui et al., 2004; Hseu et al., 2012; Shvedova et al., 2002). The comet assay (single-cell gel electrophoresis) is a rapid and sensitive fluorescence microscopic method for the detection of primary DNA damage on the individual cell level (Kim et al., 2012). Therefore, we used the comet assay to measure AAPH-induced DNA single-strand breaks in individual keratinocytes and the protective effects of lucidone. Our observations also showed that DNA was severely and systemically damaged upon the exposure to AAPH, with increases in the tail length and amount of DNA in the tails as direct evidence for single-strand DNA breakage and apoptosis. However, pretreatment with lucidone significantly eliminated the AAPH-induced single-strand DNA breaks in keratinocytes.

Several investigations have demonstrated that COX-2 expression is associated with sunburn and a large number of human inflammatory, hyperproliferative, and autoimmune diseases, including psoriasis, rheumatoid arthritis, and cutaneous lupus erythematosus (Ichihashi et al., 2009). With regard to epidermal keratinocytes, there are number of investigations demonstrating that prostaglandin synthesis is not only highly regulated but also required for skin tumor development (Maldve et al., 2000). The

exposure of keratinocytes to diverse classes of chemical tumor promoters induces the expression of COX-2 and elevates the synthesis of PGE₂ (Maldve et al., 2000), which plays a major role as a mediator of the inflammatory response. The rate-limiting enzyme in the synthesis of PGE₂ is COX-2 (Cui et al., 2004). AAPH is known to induce oxidation in biological molecules, for example, inducing lipid peroxidation in liposomes (Murase et al., 1998), and it has also been reported that treatment with such lipid peroxidation products as ROS up-regulates COX-2 expression and PGE₂ synthesis in keratinocytes (Simmler et al., 2010). A previous study demonstrated that there was no or a low level of endogenous PGE₂ and COX-2 in HaCaT cells, whereas AAPH exposure caused the up-regulation of the COX-2 protein, suggesting a role for COX-2 in PGE₂ synthesis in response to acute AAPH exposure (Cui et al., 2004). In this report, we also demonstrated that HaCaT cells exposed to AAPH exhibit increased PGE₂ production and COX-2 expression, with lucidone significantly inhibiting the AAPH-induced COX-2 expression and subsequent PGE₂ production. In addition, the over-expression of COX-2 has also been reported in various experimental models of skin inflammation and carcinogenesis, and specific inhibitors of COX-2 have been shown to suppress external stimulus-induced skin inflammation and tumor development (Wilgus et al., 2004). Thus, the present study further confirms the potential preventive effects of lucidone against AAPH-mediated inflammatory response in keratinocytes.

In resting cells, the cytoplasmic I κ B proteins, such as I κ B α , I κ B β , and I κ B ϵ , are associated with NF- κ B dimers in the cytoplasm, and stimulation with some physical or chemical stimulus leads to the activation of I κ B. Once I κ B is phosphorylated and degraded, the unbound NF- κ B molecules translocate to the nucleus and activate the transcription of genes, including COX-2 (Senthil Kumar and Wang, 2009). A previous study has also demonstrated that AAPH induces the NF- κ B pathway to stimulate the production of pro-inflammatory cytokines and pro-inflammatory enzymes, such as iNOS and COX-2, in human embryonic kidney 293T cells (Lee et al., 2009). In the present study, the exposure of keratinocytes to AAPH was found to markedly activate the transcriptional activity of NF- κ B, as confirmed by the increased nuclear export of NF- κ B using immunofluorescence analysis and western blotting. Additionally, the determination of I κ B α protein stability by Western blotting showed that AAPH treatment significantly induced I κ B α degradation, whereas the pretreatment with lucidone suppressed NF- κ B activity through the inhibition of I κ B α degradation. These results agree with our previous study, showing that lucidone significantly and dose dependently suppressed LPS-induced NF- κ B activity in murine macrophage cells (Senthil Kumar and Wang, 2009). Taken together, these data confirmed that lucidone inhibits the expression of COX-2 and, thereby, PGE₂ production through NF- κ B by reducing I κ B α degradation in AAPH-treated human keratinocytes.

It has been reported that AAPH-induced COX-2 expression requires the activation of MAPKs, including the ERK, p38 MAPK, and JNK signaling pathways (Cui et al., 2004). In the present study, we also observed that AAPH treatment increases the phosphorylation of ERK, p38 MAPK, and JNK in HaCaT cells, whereas lucidone pretreatment significantly inhibited the AAPH-induced activation of MAPKs. A similar effect of lucidone against the LPS-induced activation of ERK, p38 MAPK, and JNK was also observed in macrophages (Senthil Kumar and Wang, 2009). Furthermore, to identify the role of MAPKs in AAPH-induced COX-2 expression, we used specific inhibitors, PD98059, SB203580, and SP600125, of ERK, p38 MAPK, and JNK, respectively. The results revealed that the ERK and p38 MAPK inhibitors significantly suppressed AAPH-induced COX-2 expression, suggesting that ERK and p38 MAPK play functional role in the regulation of COX-2 expression via AAPH. However, the JNK inhibitor did not show any significant effect

against the AAPH-induced COX-2 expression, suggesting that the JNK signaling pathway is not involved in AAPH-mediated COX-2 expression in keratinocytes.

Previous studies in a variety of human cell lines have shown that generated ROS may have a potent ability to modify the –SH groups on cysteine residues in Keap1, an endogenous inhibitor of Nrf2, through ROS production (Trachootham et al., 2008). Structural activity relationship studies have revealed that phytochemicals that possess α,β -unsaturated ketone moieties could act as Michael-reaction acceptors that are able to modify the cysteine thiol residues in Keap-1 (Surh, 2003). Certain dietary phytochemicals, such as curcumin, caffeic acid phenethyl ester (CAPE), and sulforaphane, contain an α,β -unsaturated ketone moiety; therefore, these compounds could serve as potent antioxidants in biological systems (Surh, 2003). Interestingly, lucidone also contains an α,β -unsaturated ketone moiety. Therefore, we believe that the highly conserved α,β -unsaturated ketone moiety may be responsible for the antioxidant potential of lucidone; further structural activity relationship studies may confirm this hypothesis.

In conclusion, lucidone supplementation reduced AAPH-induced oxidative damage and inflammation in keratinocytes. The protective and preventive mechanism of lucidone is most likely mediated by the induction of the HO-1 gene through the up-regulation of the Nrf2 signaling pathway. Additionally, lucidone protects human keratinocytes against AAPH-induced inflammation through the suppression of NF- κ B and MAPK signaling pathways. Therefore, lucidone and *L. erythrorcarpa* could be used as accessible sources of natural antioxidants and possible food supplements, with potential applications in the pharmaceutical industry.

Conflict of Interest

The authors have no conflicts of interest to declare.

Acknowledgments

This work was supported by Grants NSC-101-2320-B-039-050-MY3, NSC-99-2320-B-039-035-MY3, CMU 100-ASIA-13, and CMU 100-ASIA-14 from the National Science Council, China Medical University, and Asia University, Taiwan.

References

- Burcham, P.C., Harkin, L.A., 1999. Mutations at G:C base pairs predominate after replication of peroxyl radical-damaged pSP189 plasmids in human cells. *Mutagen* 14, 135–140.
- Camera, E., Mastrofrancesco, A., Fabbri, C., Daubrawa, F., Picardo, M., Sies, H., Stahl, W., 2009. Astaxanthin, canthaxanthin and beta-carotene differently affect UVA-induced oxidative damage and expression of oxidative stress-responsive enzymes. *Exp. Dermatol.* 18, 222–231.
- Chao, J., Li, H., Cheng, K.W., Yu, M.S., Chang, R.C., Wang, M., 2010. Protective effects of pinostilbene, a resveratrol methylated derivative, against 6-hydroxydopamine-induced neurotoxicity in SH-SY5Y cells. *J. Nutr. Biochem.* 21, 482–489.
- Chen, W., Tang, Q., Gonzales, M.S., Bowden, G.T., 2001. Role of p38 MAP kinases and ERK in mediating ultraviolet-B induced cyclooxygenase-2 gene expression in human keratinocytes. *Oncogene* 20, 3921–3926.
- Chen, W.C., Wang, S.Y., Chiu, C.C., Tseng, C.K., Lin, C.K., Wang, H.C., Lee, J.C., 2013. Lucidone suppresses hepatitis C virus replication by Nrf2-mediated hemoxigenase-1 induction. *Antimicrob. Agents Chemother.* 57, 1180–1191.
- Cui, Y., Kim, D.S., Park, S.H., Yoon, J.A., Kim, S.K., Kwon, S.B., Park, K.C., 2004. Involvement of ERK AND p38 MAP kinase in AAPH-induced COX-2 expression in HaCaT cells. *Chem. Phys. Lipids* 129, 43–52.
- Ding, P.H., Wang, C.Y., Darveau, R.P., Jin, L., 2012. NF- κ B and p38 MAPK signaling pathways are critically involved in *Porphyromonas gingivalis* lipopolysaccharide induction of lipopolysaccharide-binding protein expression in human oral keratinocytes. *Mol. Oral. Microbiol.* <http://dx.doi.org/10.1111/omi.12010>.
- English, J.S., Dawe, R.S., Ferguson, J., 2003. Environmental effects and skin disease. *Br. Med. Bull.* 68, 129–142.
- Fan, Y.B., Lu, S.Y., Pong, L.C., 2005. A plant with great potential: the mountain pepper. *Taiwan Forestry J.* 31, 61.
- Fujiwara, N., Kobayashi, K., 2005. Macrophages in inflammation. *Curr. Drug Targets Inflamm. Allergy* 4, 281–286.

- Gilston, V., Blake, D.R., Winyard, P.G., 2000. Inflammatory mediators, free radicals and gene transcription. In: Winyard, P.G., Blake, D.R., Evans, C.H., (Eds.), *Free Radic. Inflamm*, Boston, pp. 83–98.
- Halliwell, B., 2007. Biochemistry of oxidative stress. *Biochem. Soc. Trans.* 35, 1147–1150.
- Hseu, Y.C., Chou, C.W., Senthil Kumar, K.J., Fu, K.T., Wang, H.M., Hsu, L.S., Kuo, Y.H., Wu, C.R., Chen, S.C., Yang, H.L., 2012. Ellagic acid protects human keratinocyte (HaCaT) cells against UVA-induced oxidative stress and apoptosis through the upregulation of the HO-1 and Nrf-2 antioxidant genes. *Food Chem. Toxicol.* 50, 1245–1255.
- Ichihashi, M., Ando, H., Yoshida, M., Niki, Y., Matsui, M., 2009. Photo-aging of the skin. *Anti-Aging Med.* 6, 46–59.
- Ichino, K., Tanaka, H., Ito, K., 1988. Two new dihydrochalcones from *Lindera erythrocarpa*. *J. Nat. Prod.* 51, 915–917.
- Kaspar, J.W., Nitire, S.K., Jaiswal, A.K., 2009. Nrf2: INrf2 (Keap1) signaling in oxidative stress. *Free Radic. Biol. Med.* 47, 1304–1309.
- Kim, J., Cha, Y.N., Surh, Y.J., 2010. A protective role of nuclear factor-erythroid 2-related factor-2 (Nrf2) in inflammatory disorders. *Mutat. Res.* 690, 12–23.
- Kim, K.N., Cha, S.H., Kim, E.A., Kang, M.C., Yang, H.M., Kim, M.J., Yang, H.Y., Roh, S.W., Jung, W.K., Heo, S.J., Kim, D., Jeon, Y.J., Oda, T., 2012. Neuroprotective effects of *Nannochlorophis oculata* against AAPH-induced oxidative damage in HT22 cells. *Int. J. Pharmacol.* 8, 527–534.
- Kregel, K.C., Zhang, H.J., 2007. An integrated view of oxidative stress in aging: basic mechanisms, functional effects, and pathological considerations. *Am. J. Physiol. Regul. Integr. Comp. Physiol.* 292, R18–36.
- Kundu, J.K., Surh, Y.J., 2005. Breaking the relay in deregulated cellular signal transduction as a rationale for chemoprevention with anti-inflammatory phytochemicals. *Mutat. Res.* 591, 123–146.
- Lee, E.K., Chung, S.W., Kim, J.Y., Kim, J.M., Heo, H.S., Lim, H.A., Kim, M.K., Anton, S., Yokozawa, T., Chung, H.Y., 2009. Allylmethylsulfide down-regulates X-ray irradiation-induced nuclear factor-kappaB signaling in C57/BL6 mouse kidney. *J. Med. Food* 12, 542–551.
- Liao, J.C., Deng, J.S., Chiu, C.S., Hou, W.C., Huang, S.S., Shie, P.H., Huang, G.J., 2012. Anti-inflammatory activities of *Cinnamomum cassia* constituents *in vitro* and *in vivo*. *Evid. Complement Alternat. Med.* 2012, 429320.
- Maldve, R.E., Kim, Y., Muga, S.J., Fischer, S.M., 2000. Prostaglandin E₂ regulation of cyclooxygenase expression in keratinocytes is mediated via cyclic nucleotide-linked prostaglandin receptors. *J. Lipid. Res.* 41, 873–881.
- Matsumura, Y., Ananthaswamy, H.N., 2004. Toxic effects of ultraviolet radiation on the skin. *Toxicol. Appl. Pharmacol.* 195, 298–308.
- McCulloch, C.A., Downey, G.P., El-Gabalawy, H., 2006. Signalling platforms that modulate the inflammatory response: new targets for drug development. *Nat. Rev. Drug Discov.* 5, 864–876.
- Murase, H., Moon, J.H., Yamauchi, R., Kato, K., Kunieda, T., Yoshikawa, T., Terao, J., 1998. Antioxidant activity of a novel vitamin E derivative, 2-(alpha-D-glucopyranosyl)methyl-2,5,7,8-tetramethylchroman-6-ol. *Free Radic. Biol. Med.* 24, 217–225.
- Muta-Takada, K., Terada, T., Yamanishi, H., Ashida, Y., Inomata, S., Nishiyama, T., Amano, S., 2009. Coenzyme Q10 protects against oxidative stress-induced cell death and enhances the synthesis of basement membrane components in dermal and epidermal cells. *Biofactors* 35, 435–441.
- Narayanan, B.A., Narayanan, N.K., Davis, L., Nargi, D., 2006. RNA interference-mediated cyclooxygenase-2 inhibition prevents prostate cancer cell growth and induces differentiation: modulation of neuronal protein synaptophysin, cyclin D1, and androgen receptor. *Mol. Cancer Ther.* 5, 1117–1125.
- Oh, H.M., Choi, S.K., Lee, J.M., Lee, S.K., Kim, H.Y., Han, D.C., Kim, H.M., Son, K.H., Kwon, B.M., 2005. Cyclopentenoides, inhibitors of farnesyl protein transferase and anti-tumor compounds, isolated from the fruit of *Lindera erythrocarpa* Makino. *Bioorg. Med. Chem.* 13, 6182–6187.
- Rada, B., Gardina, P., Myers, T.G., Leto, T.L., 2011. Reactive oxygen species mediate inflammatory cytokine release and EGFR-dependent mucin secretion in airway epithelial cells exposed to *Pseudomonas pyocyanin*. *Mucosal Immunol.* 4, 158–171.
- Rijnkels, J.M., Moison, R.M., Podda, E., van Henegouwen, G.M., 2003. Photoprotection by antioxidants against UVB-radiation-induced damage in pig skin organ culture. *Radiat. Res.* 159, 210–217.
- Roche, M., Tarnus, E., Rondeau, P., Bourdon, E., 2009. Effects of nutritional antioxidants on AAPH- or AGEs-induced oxidative stress in human SW872 liposarcoma cells. *Cell Biol. Toxicol.* 25, 635–644.
- Saveria, P., Mascia, F., Mariani, V., Girolomoni, G., 2006. Keratinocytes in skin inflammation. *Expert. Rev. Dermatol.* 1, 279–291.
- Schafer, M., Farwanah, H., Willrodt, A.H., Huebner, A.J., Sandhoff, K., Roop, D., Hohll, D., Bloch, W., Werner, S., 2012. Nrf2 links epidermal barrier function with antioxidant defense. *EMBO Mol. Med.* 4, 364–379.
- Scharffetter-Kochanek, K., Wlaschek, M., Brenneisen, P., Schauen, M., Blaudschun, R., Wenk, J., 1997. UV-induced reactive oxygen species in photocarcinogenesis and photoaging. *Biol. Chem.* 378, 1247–1257.
- Senthil Kumar, K.J., Hsieh, H.W., Wang, S.Y., 2010. Anti-inflammatory effect of lucidone in mice via inhibition of NF-kappaB/MAP kinase pathway. *Int. Immunopharmacol.* 10, 385–392.
- Senthil Kumar, K.J., Liao, J.W., Xiao, J.H., Gokila Vani, M., Wang, S.Y., 2012. Hepatoprotective effect of lucidone against alcohol-induced oxidative stress in human hepatic HepG2 cells through the up-regulation of HO-1/Nrf-2 antioxidant genes. *Toxicol. In Vitro* 26, 700–708.
- Senthil Kumar, K.J., Wang, S.Y., 2009. Lucidone inhibits iNOS and COX-2 expression in LPS-induced RAW 264.7 murine macrophage cells via NF-kappaB and MAPKs signaling pathways. *Planta. Med.* 75, 494–500.
- Sharma, P., Jha, A.B., Dubey, R.S., Pessarakli, M., 2012. Reactive oxygen species, oxidative damage, and antioxidative defense mechanism in plants under stressful conditions. *J. Bot.* <http://dx.doi.org/10.1155/2012/217037>.
- Shvedova, A.A., Tyurina, J.Y., Kawai, K., Tyurin, V.A., Kommineni, C., Castranova, V., Fabisiak, J.P., Kagan, V.E., 2002. Selective peroxidation and externalization of phosphatidylserine in normal human epidermal keratinocytes during oxidative stress induced by cumene hydroperoxide. *J. Invest. Dermatol.* 118, 1008–1018.
- Simmler, C., Antheaume, C., Lobstein, A., 2010. Antioxidant biomarkers from *Vanda coerulea* stems reduce irradiated HaCaT PGE-2 production as a result of COX-2 inhibition. *PLoS One* 28, e13713.
- Singh, N.P., McCoy, M.T., Tice, R.R., Schneider, E.L., 1988. A simple technique for quantitation of low levels of DNA damage in individual cells. *Exp. Cell Res.* 175, 184–191.
- Spagnoli, L.G., Bonanno, E., Sangiorgi, G., Mauriello, A., 2007. Role of inflammation in atherosclerosis. *J. Nucl. Med.* 48, 1800–1815.
- Surh, Y.J., 2003. Cancer chemoprevention with dietary phytochemicals. *Nat. Rev. Cancer* 3, 768–780.
- Svobodova, A., Psotova, J., Walterova, D., 2003. Natural phenolics in the prevention of UV-induced skin damage. A review. *Biomed. Pap. Med. Fac. Univ. Palacky. Olomouc. Czech Repub.* 147, 137–145.
- Svobodova, A., Zdarilova, A., Walterova, D., Vostalova, J., 2007. Flavonolignans from *Silybum marianum* moderate UVA-induced oxidative damage to HaCaT keratinocytes. *J. Dermatol. Sci.* 48, 213–224.
- Syed, D.N., Malik, A., Hadi, N., Sarfaraz, S., Afaq, F., Mukhtar, H., 2006. Photochemopreventive effect of pomegranate fruit extract on UVA-mediated activation of cellular pathways in normal human epidermal keratinocytes. *Photochem. Photobiol.* 82, 398–405.
- Trachootham, D., Lu, W., Ogasawara, M.A., Nilsa, R.D., Huang, P., 2008. Redox regulation of cell survival. *Antioxid. Redox. Signal.* 10, 1343–1374.
- Vessey, D.A., Lee, K.H., Blacker, K.L., 1992. Characterization of the oxidative stress initiated in cultured human keratinocytes by treatment with peroxides. *J. Invest. Dermatol.* 99, 859–863.
- Wang, S.Y., Lan, X.Y., Xiao, J.H., Yang, J.C., Kao, Y.T., Chang, S.T., 2008. Antiinflammatory activity of *Lindera erythrocarpa* fruits. *Phytother. Res.* 22, 213–216.
- Wilgus, T.A., Bergdall, V.K., Tober, K.L., Hill, K.J., Mitra, S., Flavahan, N.A., Oberyszyn, T.M., 2004. The impact of cyclooxygenase-2 mediated inflammation on scarless fetal wound healing. *Am. J. Pathol.* 165, 753–761.
- Yokozawa, T., Cho, E.J., Hara, Y., Kitani, K., 2000. Antioxidative activity of green tea treated with radical initiator 2,2'-azobis(2-amidinopropane) dihydrochloride. *J. Agric. Food Chem.* 48, 5068–5073.
- Zhang, H., Chen, T., Jiang, J., Wong, Y.S., Yang, F., Zheng, W., 2011. Selenium-containing allophycocyanin purified from selenium-enriched *Spirulina platensis* attenuates AAPH-induced oxidative stress in human erythrocytes through inhibition of ROS generation. *J. Agric. Food Chem.* 59, 8683–8690.